

# Floquet-Bloch theory and topology in periodically driven lattices

A. Gómez-León and G. Platero

*Instituto de Ciencia de Materiales de Madrid (ICMM-CSIC), Cantoblanco, 28049 Madrid, Spain*

(Dated: March 22, 2013)

We propose a general framework to solve tight binding models in  $D$  dimensional lattices driven by ac electric fields. Our method is valid for arbitrary driving regimes and allows to obtain effective Hamiltonians for different external fields configurations. We establish an equivalence with time independent lattices in  $D+1$  dimensions, and analyze their topological properties. Further, we demonstrate that non-adiabaticity drives a transition from topological invariants defined in  $D+1$  to  $D$  dimensions. Our approach provides a theoretical framework to analyze ac driven systems, with potential applications in topological states of matter, and non-adiabatic topological quantum computation, predicting novel outcomes for future experiments.

*Introduction:* Periodically driven quantum systems has been a fastly growing research in the last years. The development of effective Hamiltonians describing ac driven systems at certain regimes, has allowed to predict novel properties such as topological phases[1–3], and quantum phase transitions[4, 5] that otherwise, would be impossible to achieve in the undriven case. Therefore, the application of ac fields has become a very promising tool to engineer quantum systems. On the other hand, the obtention of effective Hamiltonians can be a difficult task, depending on the driving regime to be considered.

In this work, we provide a general framework to study periodically driven quantum lattices. By means of our approach, it is possible to solve with arbitrary accuracy their time evolution, and obtain effective Hamiltonians for the different driving regimes. We consider solutions of Floquet-Bloch form, based on the symmetries of the system, and characterize the states in terms of the quasi-energies, which are well defined for all driving regimes. The states belong to a composed Hilbert space, in which time is treated as a parameter. As we will see below, it allows to formally describe the ac driven  $D$  dimensional lattice, as analog to a time independent  $D+1$  dimensional lattice. This description enlightens the underlying structure of periodically driven systems, in which the initial Bloch band splits into several copies (Floquet-Bloch bands), where the coupling between them directly depends on the driving regime. Interestingly, the isolated Floquet-Bloch bands possess the same topological properties as the Bloch bands of the undriven system, now tuned by the external field parameters. Thus, the topological invariants for the isolated Floquet-Bloch bands can be obtained following the general classification of time independent systems (AZ classes[6–8]). However, we also demonstrate that lowering the frequency, the bands couple to each other. In that case, the topological structures are classified according to a base manifold of dimension  $D+1$ . In consequence, one can simulate higher dimensional tight binding (TB) models with exotic tunable hoppings by just coupling the system to ac electric fields.

Our approach is valid for arbitrary dimension, and it

allows to independently analyze the effect of the field amplitude and frequency. We show that the field amplitude controls the renormalization of the system parameters, while the frequency acts analogously to a DC electric field in the extra dimension. In particular, this last property relates the high frequency regime with the existence of Bloch oscillations and Landau-Zener transitions between bands[9], establishing a direct relation between diabatic regime and localization[10]. We illustrate our formalism with the analysis of an ac driven dimers chain[11–13].

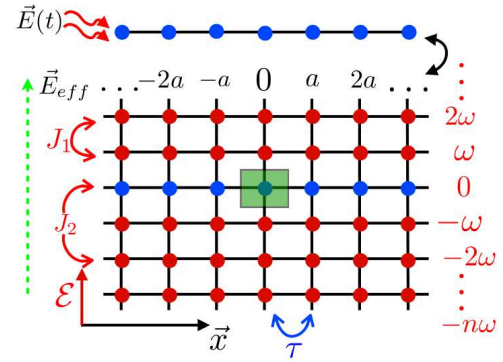


Figure 1: Schematic figure of the equivalence between a periodically driven 1D chain, and the effective time independent lattice in 2D. We plot the positions of the undressed states (blue) and their spatial distribution at sites  $ra$ ,  $r \in \mathbb{Z}$ . Each site is coupled to a set of dressed states (red color), with coupling  $\propto \tau J_p(A_0)$ , being  $p = n - m$  the difference in the number of photons between the coupled Floquet bands, and  $A_0$  the vector potential amplitude. We draw the Wigner-Seitz unit cell in 2D (green), and the effective dc electric field (see text) along the energy axis  $\mathcal{E}$  (green dotted arrow). The extra dimension  $\mathcal{E}$  arises due to the time periodicity.

*Theory:* We start by considering a Hamiltonian with lattice and time translation invariance:  $H(\mathbf{x} + \mathbf{a}_i, t + T) = H(\mathbf{x} + \mathbf{a}_i, t) = H(\mathbf{x}, t + T)$ , characterized by lattice vectors  $\mathbf{a}_i$  and time period  $T = 2\pi/\omega$ . Under these assumptions, we assume the Floquet-Bloch ansatz[14, 15]  $|\Psi_{\alpha, \mathbf{k}}(\mathbf{x}, t)\rangle = e^{i\mathbf{k} \cdot \mathbf{x} - i\epsilon_{\alpha, \mathbf{k}} t} |u_{\alpha, \mathbf{k}}(\mathbf{x}, t)\rangle$ , being  $\epsilon_{\alpha, \mathbf{k}}$  the quasi-energy for the  $\alpha$  Floquet state, and  $\mathbf{k}$  the wave-vector. The Floquet-Bloch states  $|u_{\alpha, \mathbf{k}}(\mathbf{x}, t)\rangle$

are periodic in both  $\mathbf{x}$  and  $t$ , and belong to the composed Hilbert space (Sambe space)  $\mathcal{S} = \mathcal{H} \otimes \mathcal{T}$ [16], where  $\mathcal{T}$  is the space of T-periodic functions and  $\mathcal{H}$  the Hilbert space. It defines a composed scalar product  $\langle\langle \dots \rangle\rangle = \int_0^T \langle \dots \rangle dt / T$ . In this space, the Floquet states fulfill the orthogonality condition  $\langle\langle u_\alpha(t) | u_\beta(t) \rangle\rangle = \frac{1}{T} \sum_{n,m} \int_0^T e^{i\omega(n-m)t} \langle u_{\alpha,n} | u_{\beta,m} \rangle dt = \delta_{\alpha,\beta} \delta_{n,m}$ , and the Floquet equation:

$$\mathcal{H}(\mathbf{k}, t) |u_{\alpha,\mathbf{k}}\rangle = \epsilon_{\alpha,\mathbf{k}} |u_{\alpha,\mathbf{k}}\rangle, \quad (1)$$

$$\begin{aligned} \mathcal{H}(\mathbf{k}, t) &\equiv e^{-i\mathbf{k}\cdot\mathbf{x}} (H(t) - i\partial_t) e^{i\mathbf{k}\cdot\mathbf{x}} \\ &= H_{\mathbf{k}}(t) - i\partial_t \end{aligned} \quad (2)$$

where  $|u_{\alpha,n}\rangle$  are the coefficients of the Fourier expansion in  $t$ , and  $\mathcal{H}(\mathbf{k}, t)$  the Floquet operator. We also define the Floquet-Bloch annihilation and creation operators  $\{c(t)_{\alpha,\mathbf{k}}, c^\dagger(t)_{\alpha,\mathbf{k}}\}$ . Note that the Floquet ansatz allows to map the time dependent Schrödinger equation to an eigenvalue equation, in which  $t$  and  $\mathbf{k}$  are both parameters. We propose below that an exact mapping between a D dimensional ac driven system and a D+1 undriven one can be established, in which  $\mathcal{H}(\mathbf{k}, t)$  is equivalent to a static Hamiltonian. It will allow to classify the topological invariants in terms of the mappings from the parameter space to the set of Floquet operators  $\mathcal{H}(\mathbf{k}, t)$ , being the parameter space now given by  $S^1 \times \mathbb{T}^n$ , where  $n$  is the dimension of the First Brillouin zone (FBZ).

We first define the Fourier transforms:

$$\begin{aligned} c(t)_{\alpha,\mathbf{k}} &= N^{-D/2} \sum_{j=1}^N \sum_{n=-\infty}^{\infty} c_{\alpha,j,n} e^{i\mathbf{k}\cdot\mathbf{R}_j + in\omega t} \\ c^\dagger(t)_{\alpha,\mathbf{k}} &= N^{-D/2} \sum_{j=1}^N \sum_{n=-\infty}^{\infty} c_{\alpha,j,n}^\dagger e^{-i\mathbf{k}\cdot\mathbf{R}_j - in\omega t}, \end{aligned} \quad (3)$$

where  $N$  is the number of sites in the the lattice with periodic boundary conditions and  $D$  the dimension of the undriven system. For a time dependent Hamiltonian in the dipolar approximation, the relation between undriven and driven system is given by the minimal coupling  $\mathbf{k} \rightarrow \mathbf{K}(t) = \mathbf{k} + \mathbf{A}(t)$ , where  $\mathbf{A}(t)$  is the vector potential. Equivalently, one can notice that in the undriven TB Hamiltonian, the hopping parameters  $\tau_{j,l}$  are  $k$  independent. Thus, one can obtain the time dependent TB by using the minimal coupling in the inverse Fourier transform, leading to the time dependent hoppings  $\tau_{j,l}(t) = \tau_{j,l} e^{i\mathbf{A}(t)\cdot(\mathbf{R}_j - \mathbf{R}_l)}$ , and being the Hamiltonian

$$H_{\mathbf{k}}(t) = \sum_{\alpha,\mathbf{k}} \sum_{j,l} \tau_{j,l}(t) e^{i\mathbf{k}\cdot(\mathbf{R}_j - \mathbf{R}_l)} c^\dagger(t)_{\alpha,\mathbf{k}} c(t)_{\alpha,\mathbf{k}}, \quad (4)$$

where the  $\alpha$  index labels the Floquet state, and the time dependence in the operators is included. Including the

expansion in Fourier series of  $c(t)_{\alpha,\mathbf{k}}$ , and  $c^\dagger(t)_{\alpha,\mathbf{k}}$  (Eq.3)

$$H_{\mathbf{k}}(t) = \sum_{\alpha,\mathbf{k}} \sum_{n,m} \sum_{j,l} \tau_{j,l}(t) c_{\alpha,\mathbf{k},n}^\dagger c_{\alpha,\mathbf{k},m} e^{i\kappa(t)\cdot(\rho_{n,j} - \rho_{m,l})}, \quad (5)$$

being the quadrivectors  $\kappa(t) \equiv (-t, \mathbf{k})$  and  $\rho_{n,j} \equiv (n\omega, \mathbf{R}_j)$ . Eq.5 gives a description of the time dependent Hamiltonian in terms of the time independent operators  $\{c_{\alpha,\mathbf{k},n}, c_{\alpha,\mathbf{k},n}^\dagger\}$ . Finally, the use of the composed scalar product allows to obtain the quasi-energies by diagonalization of the matrix:

$$\langle\langle u_{\alpha,\mathbf{k},n} | \mathcal{H}(\mathbf{k}, t) | u_{\alpha,\mathbf{k},m} \rangle\rangle = \tilde{\tau}_{n,m} - n\omega \delta_{n,m}, \quad (6)$$

$$\tilde{\tau}_{n,m} \equiv \frac{1}{T} \int_0^T \sum_{j,l} \tau_{j,l}(t) e^{i\kappa(t)\cdot(\rho_{n,j} - \rho_{m,l})} dt, \quad (7)$$

where  $n\omega \delta_{n,m}$  is the Fourier space representation of  $-i\partial_t$ . Eq.6 is analog to a time independent TB in D+1 dimensions with an electric field of unit intensity applied along the extra dimension, and sites labeled by  $(n, j)$  (see Fig.1). The effective electric field breaks translational symmetry in the  $\mathcal{E}$  axis, and one can differentiate two regimes: Low and high frequency.

In the low frequency regime ( $\omega \ll \tau_{j,i}$ ), it is a good approximation to neglect the effect of the time derivative in the Floquet operator (Eq.2), or equivalently, the Stark shift due to the effective electric field. Then, we restore the  $\mathcal{E}$  axis translational symmetry, and the operator can be diagonalized by Fourier transform of Eq.6 to  $t$  domain. The obtained  $\mathcal{H}(\mathbf{k}, t)$  is analog to a Hamiltonian over a D+1 compact base manifold, that we define as the First Floquet Brillouin Zone (FFBZ), parametrized by  $\{t, \mathbf{k}\} \in S^1 \times \mathbb{T}^n$  [17]. Hence, the system topology is classified according to the AZ class of D+1 static Hamiltonians. Note that if one initially assumes adiabatic evolution, the Floquet structure, the parameters renormalization by the field amplitude, and the additional dimension of the base manifold are not obtained. Thus, the topological classification is not clearly established.

For high frequency ( $\omega \gg \tau_{j,l}$ ), the effective electric field produces Bloch-Zener transitions and Bloch oscillations[9, 10], inducing localization in  $n\omega$ , and decoupling the Floquet bands. Then, Eq.6 becomes block-diagonal in Fourier space, and the effective Floquet operator time independent. In addition, it is defined over a D dimensional base manifold  $\mathbf{k} \in \mathbb{T}^n$  (FBZ). In consequence, the topological classification is given by the AZ classes for time independent systems in D dimensions. The transition from a D+1 to a D dimensional base manifold (equivalently, from the FFBZ to the FBZ), as one increases the frequency  $\omega$ , is driven by the non-adiabatic processes along the  $t$  axis[18].

Importantly, note that in general the hopping between  $n, m$  neighbors depends on the amplitude of the vector potential (Eq.7). It allows to design “effective lattices” by tuning the hoppings with the ac field[19].

*Periodically driven dimers chain:* Here we consider the case of a dimers chain coupled to an ac electric field, with hoppings  $\tau$  and  $\tau'$ , and periodic boundary conditions (Fig.2). The electric field  $E(t) = -\partial_t A(t)$ , is given by the vector potential  $A(t) = A_0 \sin(\omega t)$ , where  $A_0 \equiv qE_0/\omega$  (we fix  $q = -1$ ).

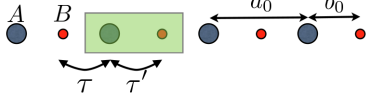


Figure 2: Schematic figure for a dimers chain with two inequivalent atoms (A, B) for unit cell (green area).  $b_0$  is the distance between A-B atoms within the same primitive cell,  $a_0$  the lattice translation vector,  $\tau'$  the hopping within the same dimer, and  $\tau$  the hopping to the next one.

By calculating  $\tilde{\tau}_{n,m}$  from Eq.7, one obtains:

$$\begin{aligned} \tilde{\tau}_{n,m} &= \tau \begin{pmatrix} 0 & \rho_F(k) \\ \tilde{\rho}_F(k) & 0 \end{pmatrix}, \\ \rho_F(k) &\equiv \lambda e^{-ikb_0} J_{n-m}(A_0 b_0) \\ &\quad + e^{ik(a_0-b_0)} J_{m-n}(A_0(a_0-b_0)), \\ \tilde{\rho}_F(k) &\equiv \lambda e^{ikb_0} J_{m-n}(A_0 b_0) \\ &\quad + e^{-ik(a_0-b_0)} J_{n-m}(A_0(a_0-b_0)). \end{aligned} \quad (8)$$

where  $\lambda = \tau'/\tau$ , and  $(n, m) \in \mathbb{Z}$ . In contrast with the undriven case, the spectrum depends on the intra-dimer distance  $b_0$ , and the hoppings are renormalized by the field amplitude. Note that for the limit of vanishing ac-field  $A_0 \rightarrow 0$ , the quasi-energies match the energies of the undriven system.

We first consider the high frequency regime ( $\omega \gg \tau, \tau'$ ), and select the Floquet band  $n = m = 0$ . In this case, the Floquet operator is block diagonal, and the system can be described by a time independent 2 by 2 matrix

$$\mathcal{H}_k^{(0)} = \tau \vec{g}(k) \cdot \vec{\sigma}, \quad (9)$$

where  $\vec{g}(k) = (\Re(\tilde{\rho}_F), \Im(\tilde{\rho}_F), 0)$  for  $n = m = 0$ , and  $\vec{\sigma} = (\sigma_x, \sigma_y, \sigma_z)$  are the Pauli matrices.

In order to compare with the case with periodic boundary conditions discussed above, we also consider a finite dimers chain with Hamiltonian  $H(t) = H_0 + qE(t)x$ , being  $H_0$  the time independent TB Hamiltonian, and  $qE(t)x$  the coupling with the electric field (details in [17]).

Fig.3 shows the quasi-energy spectrum in high frequency regime. We included in green dotted lines the regions of existence of edge states, obtained from the numerical calculation of the finite size system.

The appearance of zero energy modes is a finite size effect linked to the underlying topology of the system. The relation between them and the bulk topology is via the bulk to edge correspondence, which relates

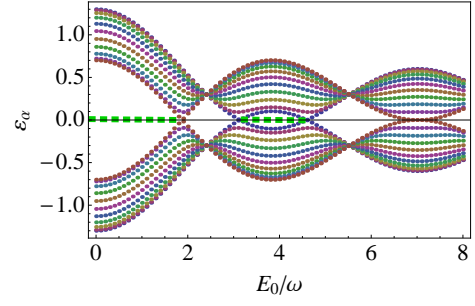


Figure 3: Quasi-energy spectrum vs  $E_0/\omega$  for  $\lambda = 0.3$ , and  $b_0 = 0$ , considering Eq.9 (high frequency). The band structure is obtained by considering 10  $k$  vectors equally spaced within the FBZ. We also included in green color the gapless modes obtained from the numerical calculation,  $\omega = 10$ . All parameters in units of  $\tau$ .

the number of zero energy modes at the boundary, carrying a topological number, with the bulk topological invariants[20]. Therefore, the calculation of the topological invariants of  $\mathcal{H}_k^{(0)}$  should predict their existence in this regime (Fig.3).  $\mathcal{H}_k^{(0)}$  belongs to the BDI class (as the one corresponding to the undriven system), with time reversal, particle-hole, and chiral symmetry[8]. In 1D, the BDI class is characterized by a winding number  $\nu_1$ , which classifies mappings  $\mathbb{T}^1 \rightarrow \mathbb{R}^2 - \{0\} \simeq S^1$ , from the FBZ to the family of Hamiltonians  $\mathcal{H}_k^{(0)}$ :

$$\begin{aligned} \nu_1 &= \oint \langle u_{\alpha,k} | i \partial_k | u_{\alpha,k} \rangle dk \\ &= \frac{\pi}{2} (1 + \text{sign}(J_0^2(y) - \lambda^2 J_0^2(x))), \end{aligned} \quad (10)$$

where  $y \equiv A_0(a_0 - b_0)$ ,  $x \equiv A_0 b_0$ , and  $|u_{\alpha,k}\rangle$  are the closed lifts of  $\mathcal{H}_k^{(0)}$ . Eq.10 shows, that in contrast with the undriven case[11], one can create non-trivial topological phases even for  $\lambda > 1$ , where the undriven system is in the trivial phase (Fig.4 left). This is an example of topology induced by the driving.

In Fig.4 (right) we plot the phase diagram corresponding to  $\lambda = 0.3$ , which correctly predicts the existence of edge states for  $b_0 = 0$  (Fig.3).

In summary, we have shown that in the high frequency regime, the topological properties can be obtained using an effective static Hamiltonian  $\mathcal{H}_k^{(0)}$ , and that they can be tuned by the field amplitude.

As we decrease  $\omega$ , the different Floquet bands couple to each other, and the isolated band picture is not accurate. In this regime, one must consider the full Floquet operator (Eq.1), which for this system is not exactly solvable. Due to the coupling between Floquet bands, two different but related effects happen as  $\omega$  is reduced: Bands inversions, and the emergence of a D+1 parameter space.

Bands inversions correspond to crossings of the bands, in which the symmetry is exchanged (e.g., it occurs

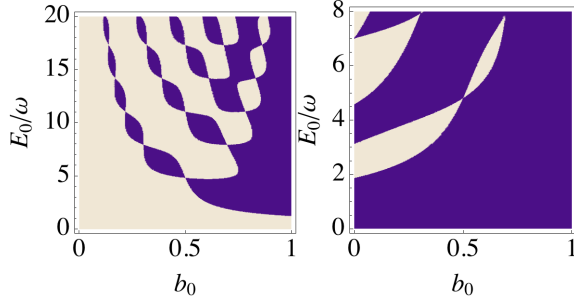


Figure 4: Topological phase diagram in the high frequency regime for an ac driven dimers chain. We considered  $\lambda = 1.5$  (left), and  $\lambda = 0.3$  (right). Dark color area means  $\nu_1 = \pi$ , and light area means  $\nu_1 = 0$ . Note that even for  $\lambda > 1$  we can induce a non-trivial topology, in contrast with the undriven case. Further, the phase diagram for  $\lambda = 0.3$  (right) agrees with the existence of edge states in Fig.3 ( $b_0 = 0$ ).

in quantum wells of HgTe/CdTe as the well thickness reaches a critical value[20]). This effect happens in ac driven systems as we decrease the frequency, because the distance between Floquet bands is proportional to  $\omega$ . If the maximum width of an isolated Floquet band, is given by  $\delta\epsilon \leq \omega$  ( $\epsilon_\alpha \in [-\omega/2, \omega/2]$ ). Then, the Floquet bands at  $\pm\omega$  close the gap when  $\omega = \delta\epsilon/2$ . As a general rule, band inversions happen for every:

$$\omega_n = \frac{\delta\epsilon}{2n}, \quad n \in \mathbb{Z}^+, \quad (11)$$

where  $\mathbb{Z}^+$  denotes the set of positive integers. Therefore, at  $\omega_n$  the  $\pm n\omega$  Floquet bands close the gap, switching between an ordinary and a topological insulating phase. For example, for a dimers chain with  $b_0 = 0$  the maximum width coincides with the undriven system band width, i.e.,  $\delta\epsilon = \delta E = 2\tau\sqrt{1 + \lambda^2} + 2\lambda$ . Then, by means of Eq.11 it is possible to track the bands inversions in terms of the undriven system[17].

For  $\omega \ll \tau, \tau'$ , a large number of bands inversions occur, being difficult to track all of them. In addition, the presence of a D+1 base manifold becomes important. In that case, one can neglect the time derivative in Eq.2, and diagonalize the operator in  $t$  domain. In that case, one obtains a 2 by 2 Floquet operator  $\mathcal{H}(k, t) \simeq H(k, t)_{\text{NN}}$  defined over the FFBZ, where  $H(k, t)_{\text{NN}}$  extends up to next nearest neighbors coupling in  $(n, m)$  (it is a good approximation for  $A_0 \leq 1$ ). However, 2D Hamiltonians in the BDI class are topologically trivial, and only the 1D topological invariant  $\nu_1$  is still non zero. It means that all changes in the topological properties will be reflected in  $\nu_1$ . In addition, for BDI Hamiltonians one can compute the winding number graphically[11], in terms of the divergences of the phase  $\phi(k, t) = \arctan(g_y/g_x)$  in the FFBZ (Fig.5), being  $g_{x,y}$  the components of the vector

$$H(k, t)_{\text{NN}} = \tau \vec{g}(k, t) \cdot \vec{\sigma}. \quad (12)$$

Note that in difference with Eq.9,  $\vec{g}(k, t)$  now depends on  $t$ , and  $\nu_1$  can be defined along the two inequivalent axis of the torus

$$\nu_1(\eta) = \frac{1}{2} \oint \frac{\partial}{\partial \mu} \phi(\mu, \eta) d\mu, \quad \mu, \eta = k, t.$$

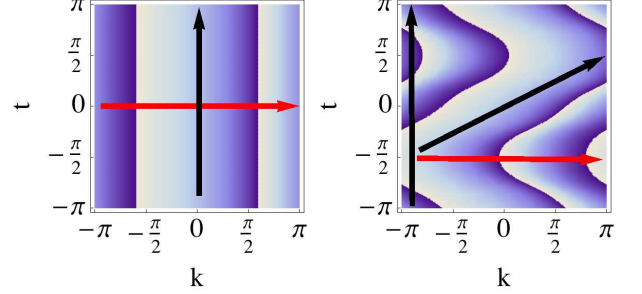


Figure 5: Plot of  $\phi(k, t)$  all over the FFBZ for  $A_0 = 0$  (left) and  $A_0 = 2$  (right). Paths parallel to  $k$  cross two discontinuities meaning  $\nu_1 = \pm\pi$  (red arrow), on the other hand, paths parallel to  $t$  have  $\nu_1 = 0$  because they wind back and forth (black arrow).

For the case of a finite chain, the existence of boundary states depends on the loops along the  $k$  axis, i.e., on  $\nu_1(t)$ [11]. In Fig.5  $\nu_1(t) = \pi$  for all  $t$ , independently of the value of  $E_0/\omega$  (trajectories always cross two discontinuities). Thus, gap inversions are not relevant for the existence of edge states in the low frequency regime, being a feature of the transition from the FBZ to the FFBZ. This can be seen numerically in the finite size system, in which zero energy modes are present independently on the gap inversions[17].

*Conclusions:* We have derived a general approach to solve periodically driven D dimensional lattices. It allows to obtain effective Hamiltonians for the different driving regimes and a complete topological classification in terms of AZ classes. We show that even for high frequency, the underlying topology of the undriven system is present due to the time periodicity. In addition, we show that at low frequency, the Floquet operator is analog to the one of a static system in D+1 dimensions, leading to interesting topological states of matter which otherwise would be inaccessible. Finally, we also described the mechanism of bands inversion in ac driven systems and its relation with the topology of the system.

We have shown a large horizon of possibilities for periodically driven systems, which in addition, can be studied experimentally e.g., by measuring the electric polarizability or the appearance of boundary states. The driving allows to simulate properties of undriven systems in higher dimensions and the obtention of new topological phases due to tunable hoppings[19]. One could also think in more exotic types of zero energy modes in the low frequency regime, as for example those in the boundary between a driven and undriven materials. Also, further

studies in the case of bichromatic ac fields could be interesting. Finally, the results in the high frequency regime can be used for non-adiabatic topological quantum computation.

We thank P. Delplace, S. Kohler, P.C.E. Stamp, and M. Büttiker for useful discussions. A.G.L. acknowledges the JAE program (MICINN) and we both acknowledge Grant No. MAT2011-24331 and the ITN Grant No. 234970 (EU).

- 
- [1] J. Inoue and A. Tanaka, Phys. Rev. Lett. **105**, 017401 (2010).
  - [2] N. Lindner, G. Refael, and V. Galitski, Nat. Phys. **7**, 490–495 (2011).
  - [3] L. Jiang et al., Phys. Rev. Lett. **106**, 220402 (2011).
  - [4] V. Bastidas, C. Emary, B. Regler and T. Brandes, Phys. Rev. Lett. **108**, 043003 (2012).
  - [5] V. Bastidas, C. Emary, G. Schaller and T. Brandes, Phys. Rev. A **86**, 063627 (2012).
  - [6] M. R. Zirnbauer, J. Math. Phys. **37**, 4986 (1996).
  - [7] A. Altland and M. R. Zirnbauer, Phys. Rev. B **55**, 1142 (1997).
  - [8] A. P. Schnyder, S. Ryu, A. Furusaki and A. W. W. Ludwig Phys. Rev. B **78**, 195125 (2008).
  - [9] C. Zener, Proc. Roy. Soc. Lond. A **145**, 523 (1934).
  - [10] N. Marzari, A. Mostofi, J. Yates, I. Souza, and D. Vanderbilt, Rev. of Mod. Phys. **84**, 1419–1475 (2012).
  - [11] P. Delplace and G. Montambaux, Phys. Rev. B **84**, 195452 (2011).
  - [12] W. P. Su, J. R. Schrieffer, and A. J. Heeger, Phys. Rev. Lett. **42**, 1698 (1979).
  - [13] S. Ryu, and Y. Hatsugai, Phys. Rev. Lett. **89**, 077002 (2002).
  - [14] M. Grifoni and P. Hänggi, Phys. Rep. **304**, 229 (1998).
  - [15] G. Platero and R. Aguado, Phys. Rep. **395**, 1 (2004).
  - [16] H. Sambe, Phys. Rev. A **7**, 2203 (1973).
  - [17] See supplementary information.
  - [18] A. Gómez-León and G. Platero, Phys. Rev. B **86**, 115318 (2012).
  - [19] W. Beugeling, J. C. Everts, and C. Morais Smith, Phys. Rev. B **86**, 195129 (2012).
  - [20] M. Hasan, C. Kane, Rev. Mod. Phys. **82**, 3045–3067 (2010).

## I. SUPPLEMENTARY INFORMATION

### S.1: Relation between undriven and ac driven Hamiltonians

For a periodic lattice, driven by an ac electric field under the dipolar approximation ( $\mathbf{A}(\mathbf{x}, t) \simeq \mathbf{A}(t)$ ), the relation between the static Hamiltonian and the ac driven Hamiltonian can be obtained by noticing that:

$$\begin{aligned}
 H &= \frac{\mathbf{p}^2}{2m} + V(\mathbf{x}), \\
 H_{\mathbf{k}} &\equiv e^{-i\mathbf{k}\cdot\mathbf{x}} H e^{i\mathbf{k}\cdot\mathbf{x}} = \frac{(\mathbf{p} + \mathbf{k})^2}{2m} + V(\mathbf{x}), \\
 H(t) &= \frac{(\mathbf{p} + \mathbf{A}(t))^2}{2m} + V(\mathbf{x}), \\
 H_{\mathbf{k}}(t) &\equiv e^{-i\mathbf{k}\cdot\mathbf{x}} H(t) e^{i\mathbf{k}\cdot\mathbf{x}} = \frac{(\mathbf{p} + \mathbf{k} + \mathbf{A}(t))^2}{2m} + V(\mathbf{x}) \\
 &= e^{-i(\mathbf{k} + \mathbf{A}(t))\cdot\mathbf{x}} H e^{i(\mathbf{k} + \mathbf{A}(t))\cdot\mathbf{x}}.
 \end{aligned} \tag{13}$$

It relies in the minimal coupling  $\mathbf{k} \rightarrow \mathbf{K}(t) = \mathbf{k} + \mathbf{A}(t)$ . Explicitly for the case of a tight binding Hamiltonian, one should notice that the hoppings can be defined as the Fourier transform of the energy:

$$\tau_{j,l} \equiv N^{-D} \sum_{\mathbf{k}} E_{\mathbf{k}} e^{-i\mathbf{k}\cdot(\mathbf{R}_j - \mathbf{R}_l)},$$

which are  $\mathbf{k}$  independent. Therefore, the inverse Fourier transform of  $\tau_{j,l}$  can encode the time dependence in the minimal coupling as:

$$H_{\mathbf{k}}(t) = N^{-D} \sum_{j,l} \tau_{j,l} e^{i\mathbf{K}(t)\cdot(\mathbf{R}_j - \mathbf{R}_l)} c(t)_{\alpha,\mathbf{k}}^\dagger c(t)_{\alpha,\mathbf{k}},$$

where the time dependent hoppings  $\tau_{j,l}(t) = \tau_{j,l} e^{i\mathbf{A}(t)\cdot(\mathbf{R}_j - \mathbf{R}_l)}$  are obtained from the time independent ones. This result relies on the same principle as the Bloch equation for a particle in a dc electric field[1].

### S.2: 1D system in low frequency regime

Let us consider as an example, a 1D chain driven by an ac electric field, where  $\omega \ll \tau_{i,j}$ , being  $\tau_{i,j}$  the hopping between sites, and  $\omega$  the frequency of the ac field. In this case, one can neglect the time derivative term of the Floquet operator, or equivalently the effective static electric field, as we described in the main text. Then, the translational symmetry along the energy axis  $\mathcal{E}$  is recovered, and one can write the Floquet operator in  $t$  domain, where it is diagonal:

$$\mathcal{H}(\mathbf{k}, t) \simeq M^{-1} \sum_{\alpha,\mathbf{k}} \sum_{n,m} \tau_{n,m} c(t)_{\alpha,\mathbf{k}} c(t)_{\alpha,\mathbf{k}}^\dagger e^{i\omega t(n-m)} \tag{14}$$

being  $M$  a normalization factor. Thus, because the Floquet operator (Eq.14) depends on the compact parameter space  $(k, t)$ , we can classify the topological properties

of  $\mathcal{H}(k, t)$  according to the AZ classification of time independent D+1 dimensional systems[2]. It classifies the mappings from the torus to the family of Floquet operators  $\mathcal{H}(k, t)$ . For example, the case of a 2 band model with Floquet operator:

$$\mathcal{H}(k, t) = \vec{h}(k, t) \cdot \vec{\sigma},$$

possess a first Chern number given by:

$$\begin{aligned} c_1 &= \int_{FBZ} \int_{-\frac{\pi}{\omega}}^{\frac{\pi}{\omega}} \hat{h}(k, t) \cdot \left( \frac{\partial}{\partial k} \hat{h}(k, t) \times \frac{\partial}{\partial t} \hat{h}(k, t) \right) dt dk \\ &= \int_{FFBZ} \hat{h}(k, t) \cdot \left( \frac{\partial}{\partial k} \hat{h}(k, t) \times \frac{\partial}{\partial t} \hat{h}(k, t) \right) dt dk, \end{aligned}$$

being the First Floquet Brillouin Zone (FFBZ) homeomorphic to a torus  $\mathbb{T}^{1+1}$ , and  $\hat{h} = \vec{h}/|\vec{h}|$ . Note that for a one dimensional time independent system,  $c_1$  would always vanish because the FBZ is given by  $\mathbb{T}^1$ . However, the increase of the parameter space dimension, due to the time periodicity, allows for higher order topological invariants.

In the particular case of a dimers chain, discussed in the main text,  $c_1 = 0$ . The reason is that the Floquet operator belongs to the BDI class in 2D. Therefore, the winding number  $\nu_1$  is the topological invariant that differentiates our system from an ordinary insulator.

### S.3 Dimers chain

#### S.3.1: Hamiltonians and topological invariants

The undriven tight binding model for nearest neighbors is given by:

$$\begin{aligned} H_k &= \begin{pmatrix} 0 & \rho(k) \\ \rho(k)^* & 0 \end{pmatrix}, \\ \rho(k) &\equiv \tau' e^{-ikb_0} + \tau e^{ik(a_0-b_0)}, \end{aligned} \quad (15)$$

$$E_{\pm} = \pm \tau \sqrt{\lambda^2 + 1 + 2\lambda \cos(ka_0)},$$

being  $\lambda \equiv \tau'/\tau$  (see Fig.2 in the main text). Importantly, the dispersion relation does not depend on  $b_0$ , and for the

condition  $b_0 = a_0/2$ , and  $\tau = \tau'$  in  $H_k$  one recovers the energy spectrum of the linear chain.

We consider the ac vector potential  $A(t) = A_0 \sin(\omega t)$ , being  $A_0 \equiv qE_0/\omega$ . By means of the minimal coupling we arrive at the time dependent Hamiltonian:

$$H_{K(t)} = \tau \begin{pmatrix} 0 & \rho(k, t) \\ \rho(k, t)^* & 0 \end{pmatrix},$$

$$\rho(k, t) \equiv \lambda e^{-i(k+A_0 \sin(\omega t))b_0} + e^{i(k+A_0 \sin(\omega t))(a_0-b_0)}.$$

In order to calculate  $\tilde{\tau}_{n,m}$  (Eq.7 in the main text), we use the identity  $J_n(x) = \frac{1}{T} \int_0^T e^{ix \sin(\omega t) - ip\omega t} dt$ , leading to:

$$\tilde{\tau}_{n,m} = \tau \begin{pmatrix} 0 & \rho_F(k) \\ \tilde{\rho}_F(k) & 0 \end{pmatrix}, \quad (16)$$

$$\begin{aligned} \rho_F(k) &\equiv \lambda e^{-ikb_0} J_{n-m}(A_0 b_0) \\ &\quad + e^{ik(a_0-b_0)} J_{m-n}(A_0(a_0-b_0)), \\ \tilde{\rho}_F(k) &\equiv \lambda e^{ikb_0} J_{m-n}(A_0 b_0) \\ &\quad + e^{-ik(a_0-b_0)} J_{n-m}(A_0(a_0-b_0)). \end{aligned} \quad (17)$$

Finally, one can obtain the matrix elements of the Floquet operator as:

$$\mathcal{H}_k^{(n,m)} = \tilde{\tau}_{n,m} - n\omega \delta_{n,m}, \quad (18)$$

where we have included the time derivative operator in Fourier space. Note that this is an infinite matrix because  $(n, m) \in \mathbb{Z}$ . In the high frequency regime ( $\omega \gg \tau, \tau'$ ), the second term in the right hand side of Eq.18 dominates, and the matrix is approximately block diagonal. Thus, we select the Floquet band  $m = n = 0$  for simplicity, being the effective Hamiltonian given by the 2 by 2 matrix:

$$\begin{aligned} \mathcal{H}_k^{(0)} &= \tau \begin{pmatrix} 0 & \rho_F^{(0)} \\ (\rho_F^{(0)})^* & 0 \end{pmatrix}, \\ \rho_F^{(0)} &\equiv \lambda J_0(A_0 b_0) + e^{ika_0} J_0(A_0(a_0-b_0)). \end{aligned} \quad (19)$$

Note that we have considered  $\rho_F^{(0)}$  in a different basis than in Eq.17. Both basis differ in a phase factor  $e^{\pm ikb_0}$ . The reason is that in order to properly obtain the topological properties we must consider the closed lifts basis[3, 4]. The quasi-energy spectrum at high frequency is ( $q = -e = -1$ ):

$$\epsilon_{\pm,k}^0 = \pm \tau \sqrt{\lambda^2 J_0^2(x) + J_0^2(y) + 2\lambda \cos(ka_0) J_0(x) J_0(y)}, \quad (20)$$

where  $x \equiv A_0 b_0$ , and  $y \equiv A_0(a_0 - b_0)$ . Fig.6 shows a comparison between the numerical calculation of a finite size system in high frequency regime (right), and

the quasi-energies obtained in the high frequency regime for the model with periodic boundary conditions, Eq.20 (left).



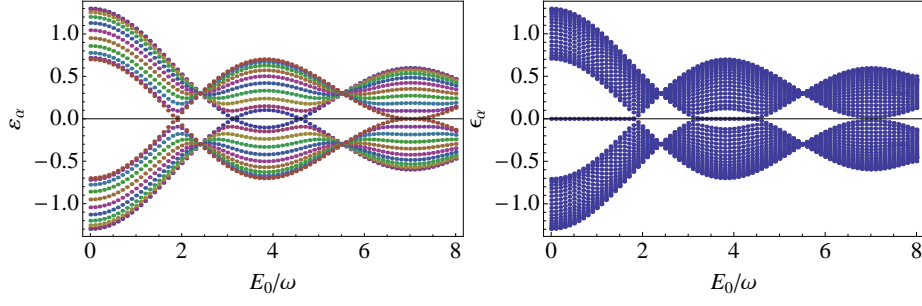


Figure 6: Quasi-energy spectrum vs  $E_0/\omega$  for  $\lambda = 0.3$ , and  $b_0 = 0$ , considering Eq.20 for the model with periodic boundary conditions (left), and the numerical solution for the finite system with 20 dimers (right). For the finite dimers chain we have considered  $n, m = 150$  sidebands and  $\omega = 10$ . Note the existence of gapless modes for a certain range of  $E_0/\omega$ . All parameters in units of  $\tau = 1$ .

Out of the high frequency regime the Floquet bands couple, and we must solve the full Floquet equation. Fig.7 shows a comparison between the model with periodic boundary conditions (left) and the finite one (right), for frequency  $\omega \simeq \tau, \tau'$ . In this regime, the Floquet bands

couple and the quasi-energies obtained in Eq.20 are no longer valid. Then, we numerically diagonalize Eq.18 for  $n, m = 15$  sidebands, and compare with the calculation for the finite system, which requires a larger number of Floquet bands in order to reach convergence ( $n, m = 85$ ).

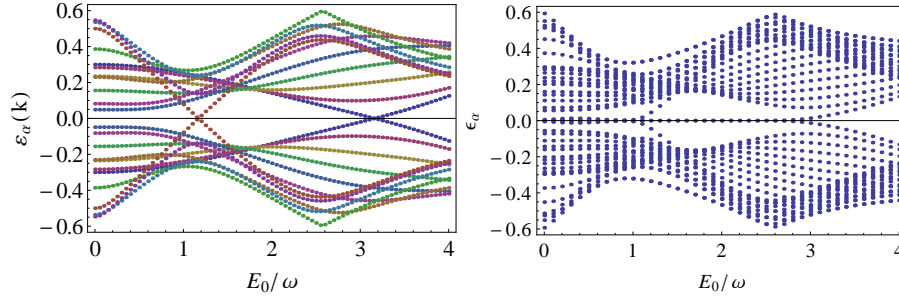


Figure 7: Quasi-energies vs  $E_0/\omega$  for  $\omega \simeq \tau, \tau'$ . We compare the model with periodic boundary conditions (left) and the finite one (right). Both models only differ in the finite size effects. The periodic boundary model has considered  $m, n = 15$  and up to fifteen order coupling, while the finite size model has considered  $m, n = 85$ . Parameters  $\omega = 1.2$ ,  $\lambda = 0.5$ , and  $b_0 = 0$  (all parameters in units of  $\tau = 1$ ).

The full Floquet operator in time domain is given by

$$(H(k, t) - i\partial_t)|u_{\alpha, k}\rangle = \epsilon_{\alpha, k}|u_{\alpha, k}\rangle. \quad (21)$$

For the calculation of  $\mathcal{H}(k, t)$ , the coupling between different Floquet bands depends on the amplitude of the vector potential. If we assume  $A_0 \leq 1$ , we can neglect the contributions from  $J_{p>2}(A_0)$ , leading to a Hamiltonian up to next nearest neighbors:

$$H(k, t)_{\text{NN}} = \tau \begin{pmatrix} 0 & \rho_F(k, t) \\ \rho_F(k, t)^* & 0 \end{pmatrix}, \quad (22)$$

$$\rho_F(k, t) \equiv \lambda J_0(x) + 2i\lambda J_1(x) \sin(\omega t) + 2\lambda J_2(x) \cos(2\omega t) + e^{ika_0} J_0(y) - 2e^{ika_0} (iJ_1(y) \sin(\omega t) - J_2(y) \cos(2\omega t)),$$

which, in the limit  $A_0 \rightarrow 0$  becomes the energy dispersion of the undriven system.

Eq.21 is not exactly solvable for the time dependent Hamiltonian  $H(k, t)_{\text{NN}}$  (Eq.22). However, for frequency values  $\omega \ll \tau, \tau'$  we can neglect the time derivative, such that  $\mathcal{H}(k, t) \simeq H(k, t)_{\text{NN}}$ . Then, Eq.21 describes an eigenvalue equation, and we can classify the mappings  $(k, t) \rightarrow \mathcal{H}(k, t)$ , from the FFBZ to the set of Floquet operators:

$$\mathcal{H}(k, t) = \tau \vec{g}(k, t) \cdot \vec{\sigma}. \quad (23)$$

The calculation of the first Chern number using Eq.23 gives  $c_1 = 0$ , because the Hamiltonian belongs to the BDI class. However, we can calculate the winding number

$\nu_1$  along the two inequivalent directions of the 2-torus  $k$  and  $t$  as:  $\nu_1(\eta) = \frac{1}{2} \oint \frac{\partial}{\partial \mu} \phi(\mu, \eta) d\mu$ , where  $\mu, \nu = k, t$ ,  $\phi(k, t) \equiv \arctan\left(\frac{g_y}{g_x}\right)$ , and  $g_{x,y}$  are the components of the vector  $\vec{g}(k, t)$  in Eq.23. As we discussed in the main text, in this case  $\nu_1(t) = \pi$  for all  $t$ , and  $\nu_1(k) = 0$  for all  $k$ .

In the present example of a dimer chain, the existence

of topologically protected states at the boundary of the chain is related with the loops along  $k$ , i.e., with the winding number  $\nu_1(t)$ . Hence,  $\nu_1(t) = \pi$  for all  $t$  means the existence of boundary states for all  $t$ , independently of the value of  $A_0$ , as far as we are in the low frequency regime (see Fig.8).

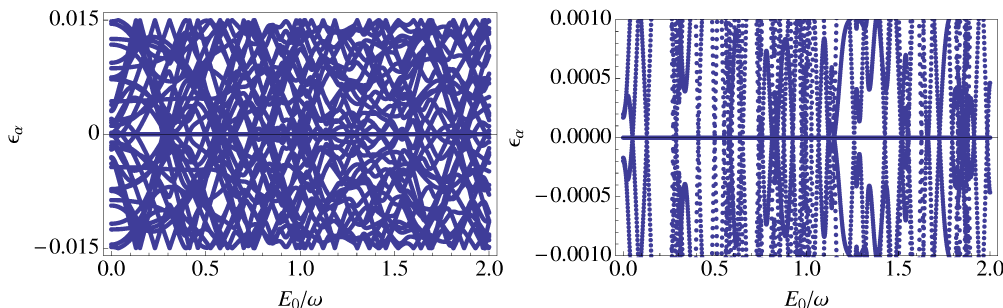


Figure 8: (Left) Quasi-energy spectrum within  $(-\omega/2, \omega/2)$  for a finite dimers chain in the low frequency regime ( $\omega \ll \tau, \tau'$ ). Right plot shows a zoom of the zero energy mode. The plots show a large number of crossings between the quasi-energies. However, the existence of zero energy modes is not affected by these crossings, and they exists for all values of  $E_0/\omega$ . We have considered a finite chain of 20 dimers,  $n, m = 105$ ,  $\omega = 3.10^{-2}$ , and  $\lambda = 0.3$  in units of  $\tau$ .

### S.3.2: Bands Inversions

Bands inversions in periodically driven lattices are produced due to the coupling between different Floquet bands as we decrease the frequency. They change the topological properties of the system by opening and closing the gap. Fig.9 shows the band structure of the dimers chain for different values of  $\omega$ . The exact crossings between conduction and valence band in this model are critical points for a topological phase transition, as the appearance/disappearance of boundary states demonstrate. While the critical points for  $\omega = 2$  (Fig.9 left)

at  $E_0/\omega \simeq 1.5$ , and 4.5 are almost fixed as we decrease the frequency, the critical point at  $E_0/\omega \sim 2.8$  shifts to the left as the frequency is lowered (Fig.9 center and right). It reaches the origin at  $\omega_1 = 1.3$  and vanishes modifying the phase diagram. Importantly, the shift of the critical points depends on the band structure of the system under consideration (the critical points can disappear at the origin, or new ones can show up). However, the gap always closes for  $\omega_n$ , independently of the critical points dynamics (being  $\omega_n \equiv \delta\epsilon/n\omega$ ,  $n \in \mathbb{Z}^+$ , and  $\delta\epsilon$  the maximum thickness of the Floquet band).



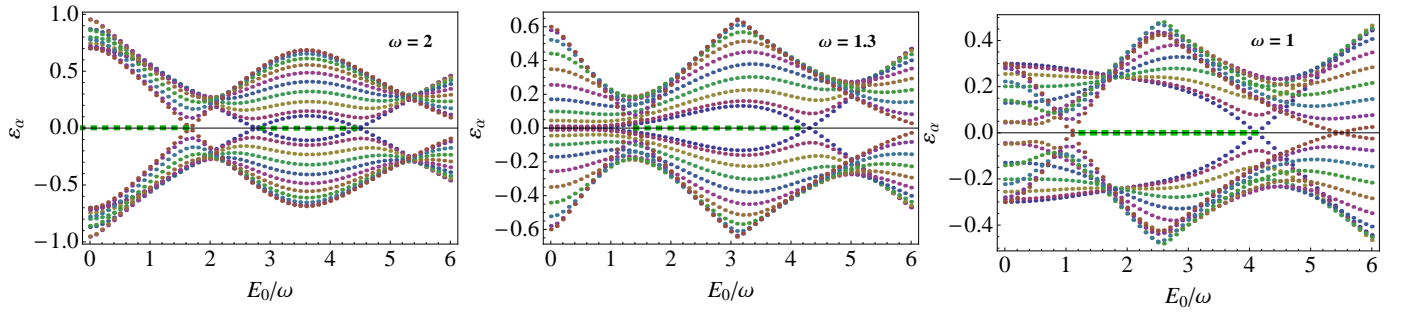


Figure 9: Quasi-energies vs  $A_0 = E_0/\omega$  for different frequencies considering periodic boundary conditions. In dotted green color we plot the boundary states, which has been obtained using a finite tight binding model. Left figure shows the quasi-energies for  $\omega = 2$ , where the bands are not inverted. The center figure shows the quasi-energies for the critical value of  $\omega_1 = 1.3$  at which the Floquet bands that belong to  $\pm\omega$  close the gap at  $A_0 = 0$ . The right figure considers a lower frequency ( $\omega = 1$ ) where the gap is reopened. Importantly, the comparison between left and right figures shows that the order in which the boundary states appear as a function of  $A_0$  is inverted.

- 
- [1] F. Bloch, Z. Phys. **52**, 555-600 (1929).
  - [2] A. P. Schnyder, S. Ryu, A. Furusaki and A. W. W. Ludwig  
Phys. Rev. B **78**, 195125 (2008).

- 
- [3] A. Bohm, A. Mostafazadeh, H. Koizumi, Q. Niu, and J. Zwanziger, The Geometric Phase in Quantum Systems (Springer, Berlin, 2003).
  - [4] C. Bena and G. Montambaux, New Journal of Physics **11**, 095003 (2009).